

Recombinant Rhodostomin Substrates Induce Transformation and Active Calcium Oscillation in Human Platelets

Hsin-Hou Chang, Chi-Hung Lin, and Szecheng J. Lo¹

Institute of Microbiology and Immunology, National Yang-Ming University, Taipei, 11221 Taiwan, Republic of China

Platelet activation has been a focus of numerous studies in normal and abnormal states. Morphological changes and calcium signals found with activated platelets *in vitro* have been well characterized. However, the rate of cell spreading on substrates and the frequency of calcium oscillation within individual platelets upon activation have not yet been reported. In this study, we first examined the ability of a recombinant fusion protein of rhodostomin (GST-rhodostomin), a snake disintegrin containing an Arg-Gly-Asp (RGD) motif, to activate platelets when GST-rhodostomin served as a substrate. Four aspects of platelet activities induced by immobilized GST-rhodostomin and fibrinogen were analyzed in parallel. Examinations of (1) translocation of P-selectin from intracellular compartments to the plasma membrane, (2) platelet adhesion to and spreading on substrates, (3) platelet contact pattern on substrates, and (4) the degree of phosphorylation of focal adhesion kinase in platelets indicated that GST-rhodostomin was a better substrate for platelet activation than fibrinogen. Analysis of the rate of platelet spreading on GST-rhodostomin was examined by time-lapsed video microscopy. The spreading rate averaged 0.43 $\mu\text{m}/\text{minute}$, while cell spreading averaged 0.22 $\mu\text{m}/\text{minute}$ when platelets were plated on fibrinogen and treated with thrombin. A newly developed method, using time-lapsed microscopy and the Metamorph program, was used to analyze calcium signals within platelets. We found that platelets on GST-rhodostomin evoked calcium oscillation at a frequency of 4.77 spike/cell/minute vs 2.76 spike/cell/minute on fibrinogen. The results of cell spreading and calcium oscillation were consistent with the results of microscopic and biochemical assays. We therefore conclude that the determination of the rate of platelet spreading and the frequency of calcium oscillation within platelets performed in this study provides more quantitative parameters for measuring platelet activities. Our results also suggest that GST-rhodostomin might potentially be used as a probe to dissect the molecular mechanisms underlying the kinetic processes of platelet activation.

anisms underlying the kinetic processes of platelet activation. © 1999 Academic Press

Key Words: adhesion; disintegrin; FAK; lamellipodia; P-selectin; video microscopy.

INTRODUCTION

Human platelets play key roles in mediating physiological hemostasis and pathological thrombosis [1, 2]. Normally, these tiny (in average 2 μm in diameter), anucleate disc-shaped cells move freely in the blood stream. At sites where vascular injury occurs, the platelets may bind to the exposed subendothelial matrix; then through complex intracellular signaling pathways, the bound cells are activated and typically exhibit a series of secretion and transformation activities that leads to platelet plug formation [1, 3]. Morphological transformation of platelets related to this coagulation event has been studied by an *in vitro* system for decades [4–8]. The kinetic processes and signaling mechanisms involved in platelet adhesion and spreading are well characterized, i.e., activation of protein kinase, elevation of calcium concentration, and reorganization of the cytoskeleton [4, 9–13]. However, no detailed measurements of the platelet spreading rate and of the frequency of calcium oscillation within platelets have been reported.

It is generally believed that fibrinogen, a blood coagulant protein (factor I), and its receptor, the integrin $\alpha_{\text{IIb}}\beta_3$ (GPIIb/IIIa), play an essential role in platelet aggregation in solution and in cell adhesion and spreading on substrates [14, 15]. Fibrinogen cannot bind to the integrin $\alpha_{\text{IIb}}\beta_3$ of resting platelets until platelets are activated by agonists, such as thrombin and ADP [16, 17]. It is thought that these agonists can induce an “inside-out” signal of the platelet that renders conformation and/or affinity changes in the integrins [18–21]. These “activated” integrins are then capable of binding to the tripeptide Arg-Gly-Asp (RGD) motif of fibrinogen in a bivalent cation-dependent manner [22, 23] and elicit the “outside-in” signals to exert various activities within platelets [9–13].

¹ To whom correspondence and reprint requests should be addressed. Fax: 886-2-28212880. E-mail: losj@ym.edu.tw.

Recently, a newly classified disintegrin family derived from snake venoms [24, 25] has been employed in studying the mechanism of anticoagulation. Unlike fibrinogen, disintegrins can directly bind to nonactivated platelets, which provide an alternative view in studying signal transduction in platelets. However, due to the small molecular weight of disintegrins and their low efficiency of coating on plates, they have never been used as substrates for studying platelet adhesion. Rhodostomin is a member of the disintegrin family which is also known as kistrin [26]. It consists of 68 amino acids, including 12 cysteine residues, and can inhibit platelet aggregation by interfering in the binding between integrin $\alpha_{IIb}\beta_3$ and fibrinogen [27–29]. Previously we have used the recombinant rhodostomin (glutathione *S*-transferase fused with rhodostomin, GST–rhodostomin) to demonstrate inhibition of thrombin-induced platelet aggregation in solution as well as induction of platelet adhesion and spreading as an adhesive substrate [30, 31]. In this study we further demonstrate that GST–rhodostomin is an ideal substrate for activating platelets, which allow us to measure and differentiate the rate of platelet spreading and the frequency of calcium oscillation within platelets by time-lapse video microscopy.

MATERIALS AND METHODS

Preparation of GST–rhodostomin. The synthesis of GST–rhodostomin fusion proteins (containing either RGD or RGE sequence motifs) using *Escherichia coli* strain RR1 was as described [30]. Briefly, bacteria containing expression plasmids were grown in 5 or 100 ml of LB medium supplemented with 50 $\mu\text{g/ml}$ ampicillin while vigorously shaken at 37°C until $A_{500\text{nm}}$ reached 0.3–0.5. Production of GST–rhodostomin was induced by addition of 0.5 mM IPTG to the medium for 1–3 h. The resulting fusion proteins were further purified by glutathione affinity chromatography and analyzed by 15% SDS–PAGE as described [32, 33].

Preparation of human platelets. Washed platelets were obtained from healthy donors under no medication and prepared as described [30, 31]. Briefly, fresh human blood drawn from the forearm vein was immediately mixed with 1/6 vol of acid–citrate–dextrose (ACD) anticoagulant and then centrifuged at 200g for 15 min. The supernatant containing the platelet-rich plasma (PRP) portion was collected and mixed with 5 mM EDTA and then centrifuged at 1000g for 12 min at room temperature. The resulting platelet pellets were resuspended in calcium-free Tyrode's buffer containing 0.35% BSA, 50 unit/ml heparin, and 1 unit/ml apyrase (Sigma, St. Louis, MO) and incubated at 37°C for 20 min. The cell suspensions were spun down again and then resuspended in Tyrode's buffer containing 1 mM calcium. The concentration of platelet suspension was adjusted to around 3.5×10^8 cell/ml before use. Note that since mechanical force associated with the preparation procedures alone might activate the platelet, care was taken in this study to minimize the "nonspecific platelet activation" to <5% of the final platelet population.

Immunofluorescence staining of P-selectin. The suspended platelets were treated with GST–rhodostomin (4.0×10^{-8} M), fibrinogen (20 $\mu\text{g/ml}$), or thrombin (0.01 NIH unit/ml) for 30 min before being spun down and fixed with 4% formaldehyde in phosphate buffer. These fixed platelets were incubated with anti-P-selectin antibody

(CD62P; Seratec, Oxford, England) for 1 h, followed by FITC-conjugated secondary antibodies, and observed under both DIC and fluorescence microscopy. Since no permeabilization step was taken during the staining procedures, the fluorescence signals obtained represent only the expression of P-selectin on the plasma membrane. Similar protocols were performed on platelets plated onto either GST–rhodostomin- or fibrinogen-coated substrates for 15 min.

Adhesion assay and scanning electron microscopy. Methods for the cell attachment assay were described previously [30, 31]. Freshly prepared nonactivated blood platelets were incubated for 15 min with coverslips coated with various amounts of GST–rhodostomin fusion proteins or fibrinogen and then washed three times with PBS. These cells were then fixed with glutaraldehyde and subjected to a series of alcohol dehydration, critical point drying procedures, and gold coating [34] and observed under a Joel scanning electron microscope at 15 kV (Model JSM-5300). At least five different areas were randomly selected for photography at each magnification; representative data are shown.

Interference reflection microscopy. Degrees of apposition between the cell and substrate were analyzed using interference reflection microscopy (IRM) as previously described [35, 36]. IRM was typically performed on living cells; however, some IRM observations were made on fixed cells to access intracellular F-actin distribution. In these experiments, platelets plated on rhodostomin- or fibrinogen-coated coverslips were fixed with 4% formaldehyde for 30 min at room temperature, extracted with 0.5% Triton X-100 in the fixative, and stained with rhodamine–phalloidin. Simultaneous epifluorescence and interference reflection microscopy was performed using a laser scanning confocal microscope (Leica TCS-NT, Heidelberg, Germany).

Analysis of FAK phosphorylation in platelets. Platelets adhered to GST–rhodostomin or fibrinogen plates were collected and dissolved with RIPA buffer containing 10 mM Tris–HCl, pH 7.2, 1 mM EDTA, 1 mM PMSF, 10 mM sodium orthovanadate, 10 mM NaF, 1% Triton X-100, 1% sodium deoxycholate, and 0.1% SDS. The cell extracts were then immunoprecipitated with protein A–Sepharose beads conjugated with anti-FAK antibodies (Transduction Laboratory, Lexington, KY). The beads and associated immunocomplex proteins were then subjected to SDS–PAGE analysis. The resulting protein profile was transferred to a nitrocellulose membrane and probed with anti-phosphotyrosine antibodies following standard Western blotting procedures [37]. The same nitrocellulose membrane, after washing with mercaptoethanol to remove previous blotting complexes, was used again for anti-FAK immunoblotting [38, 39]. A combination of horseradish peroxidase and the ECL system was used for detection following methods recommended by the manufacturer (Amersham, Buckinghamshire, England).

Time-lapse video microscopy and image processing. Acid-washed coverslips were coated with GST–rhodostomin or fibrinogen (20 $\mu\text{g/ml}$) as described and used to assemble the custom-made perfusion chambers [40]. About 200 ml of cell suspension was added to the chamber and incubated for 15 min before microscopic observation. Time-lapse recording of living platelets was performed using a Nikon Diaphot 300 inverted microscope and the Metamorph program (Universal Imaging Corp., West Chester, PA). The processed images were recorded on an optical memory laser disk (Sony Model LVR-5000) and redigitized for data analysis and image processing prior to dye-sublimation printer output (Kodak XLS 8600PS).

Calcium imaging. To perform calcium imaging techniques, freshly prepared human platelets were incubated with 10 mM membrane-permeable Calcium Green I-AM ester (Molecular Probes, Eugene, OR) in the calcium-free buffer containing apyrase for 30 min, as previously described [41]. After dye loading, cells were resuspended in Tyrode's buffer containing 1 mM calcium. The changes of intracellular calcium concentration were observed under a fluores-

cence microscope and recorded with a signal intensified tube (SIT) camera (Hamamatsu C-2400). Image sequences were recorded at video rates for at least 30 s in each experiment. No significant fluorescence photobleaching (<5% decay) was noted during the recording period. Analysis of calcium signal kinetics was done using the Metamorph program. About 150 cells (per image) in each experiment were first chosen and marked. The image sequence (30 frames/s for 30 s) was then resampled and digitized at five-frame/s intervals, typically resulting in 150 pictures per sequence. The changes of fluorescence intensity, indicative of changes in intracellular calcium concentration, were measured; the rate of change per unit of time (the slope) was then derived and plotted as a function of time. After applying a rolling average of three to the data to eliminate nonspecific fluctuation of calcium signals that is not obvious to online observation under the fluorescence microscope, we could then count the calcium spikes and calculate the frequency of calcium oscillation as spikes/cell/minute.

RESULTS

Platelets Were Activated by Substrate-Bound but Not Soluble GST-Rhodostomin

GST-rhodostomin in solution, although an effective inhibitor of platelet aggregation, could not induce obvious shape changes in platelets, whereas immobilized GST-rhodostomin could effectively cause platelet attachment and spreading [30, 31]. To address the activation status of platelets in these different rhodostomin treatments, we examined the degree of P-selectin translocation from intracellular compartments to the cell membrane [42]. The amounts of P-selectin expressed on the cell surface were accessed by immunofluorescence staining on cells that were fixed but not permeabilized. When suspended platelets were treated with either soluble fibrinogen (Fig. 1B) or GST-rhodostomin (Fig. 1D), neither of the platelets showed significant P-selectin staining. Note that addition of thrombin, which is known to activate platelets, caused profound redistribution of P-selectin to the cell surface (Fig. 1F). Since thrombin treatments also caused platelet aggregation, fewer single cells were found on the thrombin-treated plates (Fig. 1E) than on fibrinogen- or rhodostomin-treated samples (Figs. 1A and 1C, respectively).

We also examined the degree of P-selectin translocation on cells interacting with immobilized fibrinogen (Fig. 2A) or GST-rhodostomin (Fig. 2B). Platelets plated on fibrinogen substrates exhibited limited exposure of P-selectin on the surface (Fig. 2A); in contrast, the cells bound to the GST-rhodostomin substrate demonstrated not only fully spread conformations (see below), but also high levels of P-selectin on the plasma membranes (Fig. 2B). These results suggest strongly that immobilized, but not soluble, GST-rhodostomin could activate human platelets.

GST-Rhodostomin Substrates Induced Platelet Adhesion and Transformation in a Dose-Dependent Manner

We then employed scanning electron microscopy (SEM) to further characterize platelet adhesion and transformation on different substrates. In one set of experiments, freshly prepared human platelets plated on substrates coated with different concentrations of GST-rhodostomin were processed for SEM examination. Representative fields of cells interacting with increasing concentrations of GST-rhodostomin substrates were shown (Fig. 3). Note that cells plated on 1.6 and 8.0×10^{-9} M GST-rhodostomin (Figs. 3A and 3B, respectively) were mostly round shaped, with some protruding filopodia, while the majority of platelets plated on higher concentrations of recombinant protein (4.0×10^{-8} and 2.0×10^{-7} M, see Figs. 3C and 3D, respectively) exhibited fully spread (pancake) conformations.

To quantify the correlation between substrate coating and degree of cell spreading, we randomly selected 100 cells from 5 SEM fields under each experimental condition and then calculated the number of fully spread ($>5 \mu\text{m}$) cells relative to the total adherent cells. As shown in Table 1, the percentage of fully spread cells increased from 2.3% on the 1.6×10^{-9} M plate to over 90% when 2.0×10^{-7} M GST-rhodostomin was used. At concentration of 4.0×10^{-8} M, about 78% of the adherent cells were fully spread; this treatment was typically used for substrate coating in the following experiments. As expected, only a few, if any, platelets were disc shaped on BSA-coated substrates (Fig. 4C). Fibrinogen substrate could not directly induce platelet transformation in most nonactivated platelets (Fig. 4B), in contrast to the robust effects of rhodostomin (Fig. 4A).

Degrees of Adherence Correlated with Morphogenetic Effects

Using the cell attachment assay, we found that the binding efficiency of platelets to GST-rhodostomin substrates was higher than that to fibrinogen-treated surfaces. To further evaluate cell-substrate interactions, we used IRM to examine the extent of cell-substrate association. In a typical IRM image, dark areas indicate closer apposition between two optical media of different refractive indexes (in this case, the coverglass substrate and the ventral plasma membrane of the cell), whereas light areas indicate relatively wide distances [35, 36]. We monitored living cells under IRM (data not shown), and the results were not different from the data taken from fixed cells (Figs. 5B and 5D). To correlate the IRM pattern with intracellular F-actin distributions, we stained the same cells

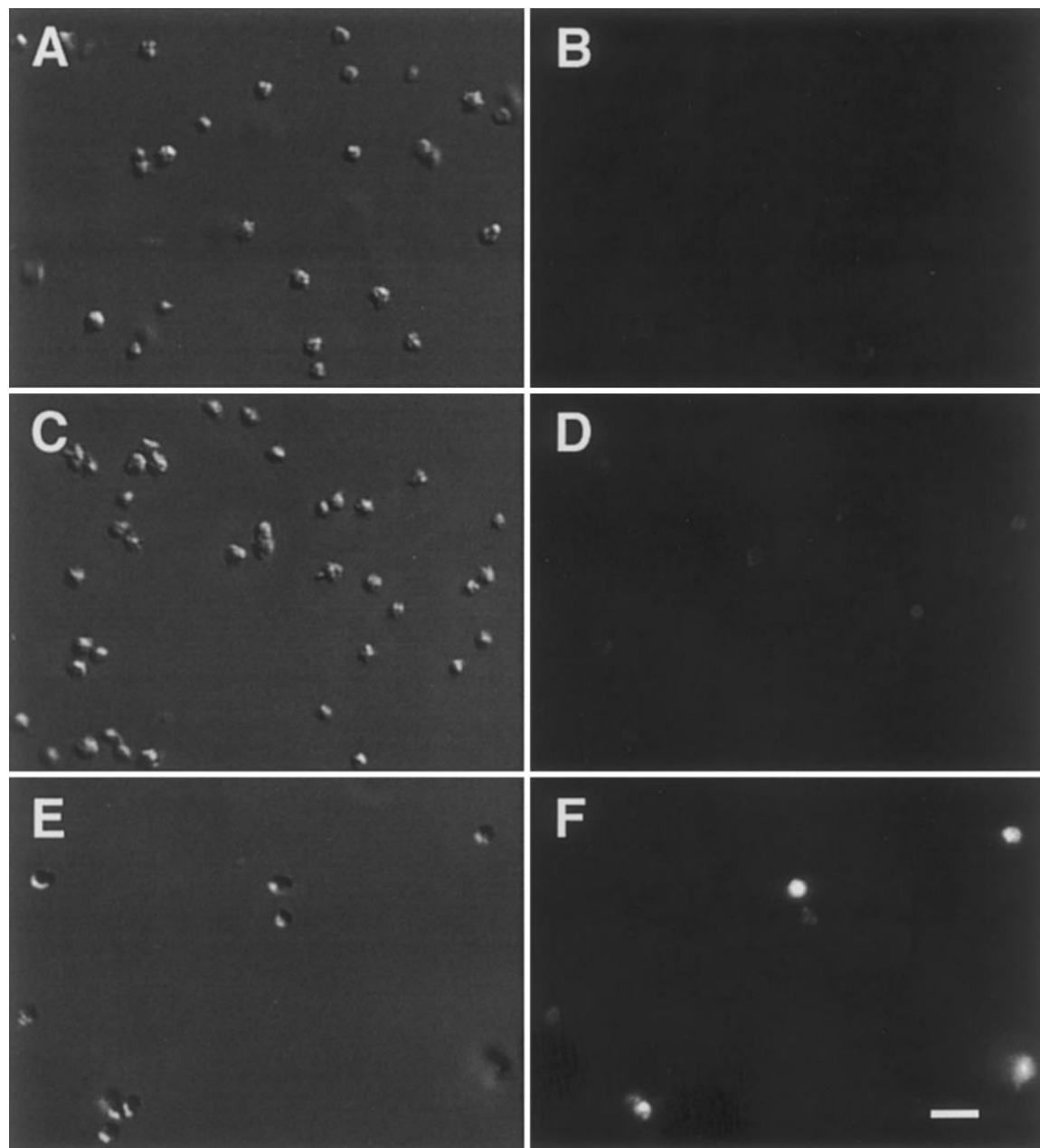


FIG. 1. Soluble GST-rhodostomin could not induce translocation of P-selectin. Human platelets in suspension were treated with soluble fibrinogen (A, B), GST-rhodostomin (C, D), or thrombin (E, F) for 30 min before harvest. These cells were fixed but not permeabilized and then processed with standard immunofluorescence staining procedures to reveal the presence of P-selectin on the plasma membrane. The same fields were observed under DIC (A, C, E) and fluorescence microscopy (B, D, F). Note that significant translocation of P-selectin occurred when cells were treated with thrombin. Much fewer single cells were found in the thrombin plate than the fibrinogen or GST-rhodostomin plates because thrombin treatments caused profound cell aggregation. Scale bar, 5 μm .

with rhodamine-phalloidin and took IRM and fluorescence images simultaneously under a confocal microscope. A typical example of these experiments is shown in Fig. 5. Most cells on fibrinogen plates were round, with only a few filopodia that stained strongly with rhodamine-phalloidin (arrowhead, Fig. 5A). These

cells were not tightly adherent to the substrate and their filopodia showed speckled gray regions, also indicating loose attachment to the plate (arrowhead, Fig. 5B). Cells plated on GST-rhodostomin plates, on the other hand, were mostly flat, with extended lamellae containing rich networks of actin filaments (Fig. 5C).

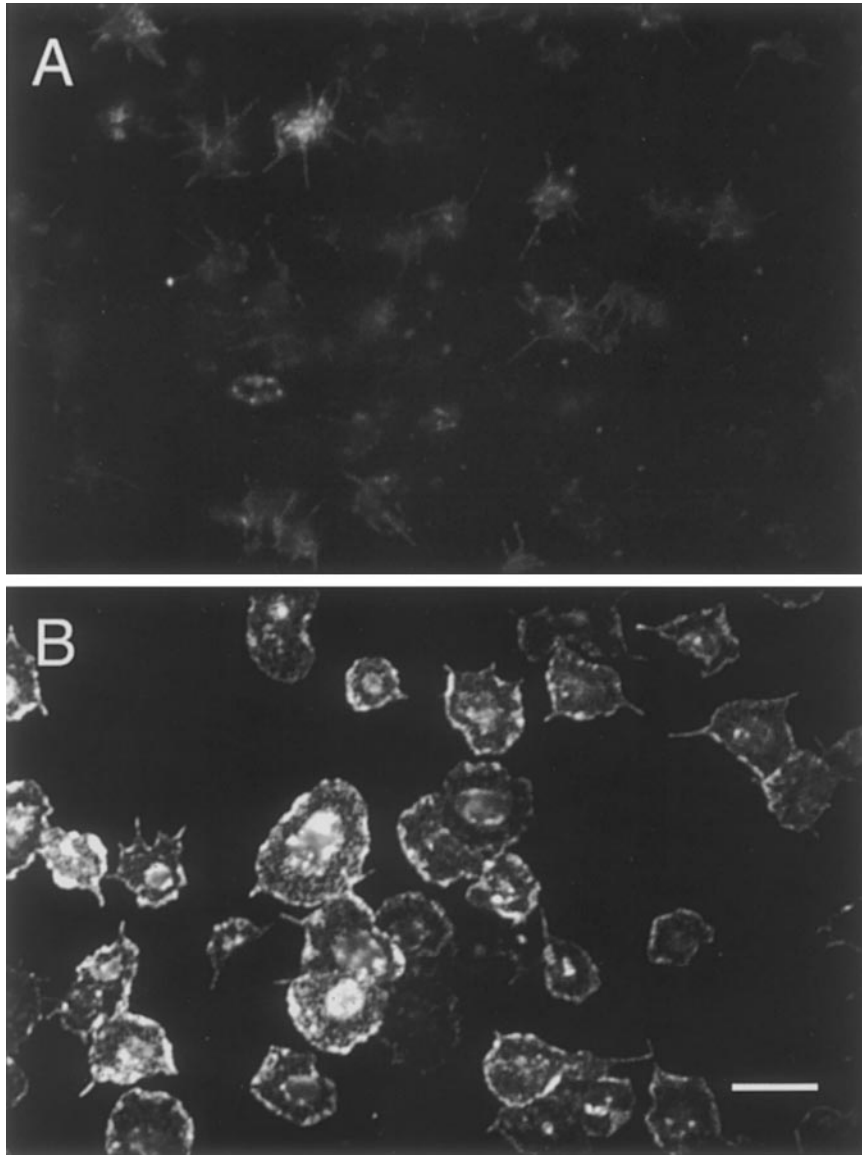


FIG. 2. Substrate effects on P-selectin translocation from the internal store to the cell membrane. Platelet cells were plated on (A) fibrinogen- or (B) GST-rhodostomin-coated substrates for 15 min before being processed with immunofluorescence staining to visualize P-selectin distribution. Most cells plated on GST-rhodostomin plates exhibited fully spread conformations and high concentrations of P-selectin on the membrane compared to those on the fibrinogen plates. Scale bar, 5 μm .

The associations between the cells and the rhodostomin substrate were so close that most of the cell-covered areas appeared dark under IRM optics (Fig. 5D).

FAK Was Highly Phosphorylated during Platelet Transformation

We also looked at another feature of cell spreading, the level of phosphorylation of FAK proteins, which is also used as a hallmark for platelet activation [39, 43]. A combination of immunoprecipitation and Western

blot analysis was performed, and a typical result is shown in Fig. 6. Using anti-phosphorylated tyrosine antibody as a probe (Fig. 6A), we found that FAK proteins from thrombin-treated platelets were highly phosphorylated (lane 1), whereas FAK proteins from nonactivated platelets were not (lane 2). In cells interacting with GST-rhodostomin, a band representing phosphorylated FAK was noted (lane 3). In contrast, little or no phosphorylated FAK was revealed in platelets plated on fibrinogen (lane 4). The level of FAK phosphorylation, however, was at least three times

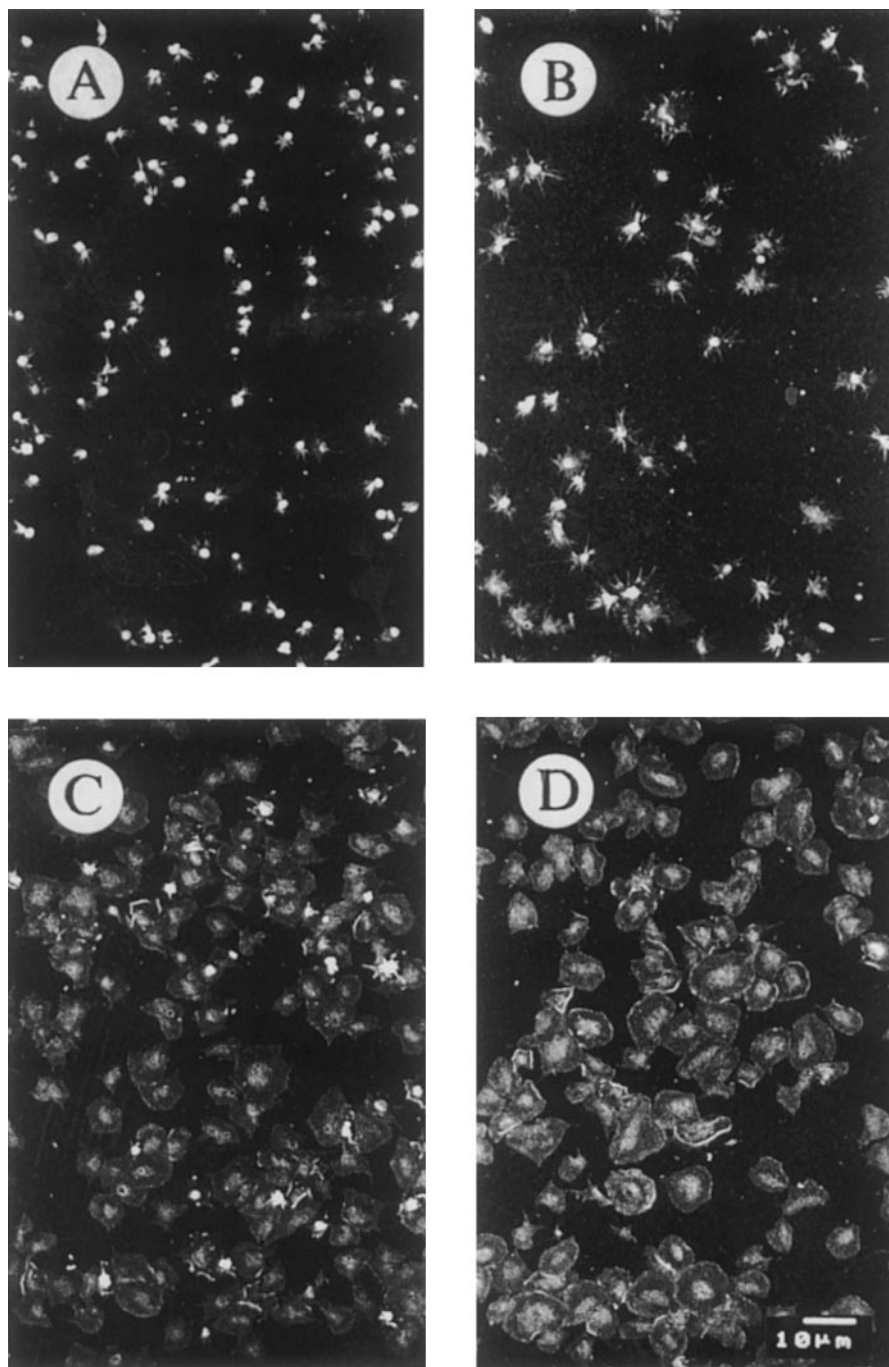


FIG. 3. SEM images of human platelets plated on recombinant rhodostomin-coated substrates. Platelet cells were plated on substrates coated with different concentrations of GST-rhodostomin (1.6×10^{-9} M, 8.0×10^{-9} M, 4.0×10^{-8} M, and 2.0×10^{-7} M in A–D, respectively) for 15 min before SEM observation. Note more cells exhibiting flattened conformations as the concentration of rhodostomin used for substrate coating increased (see also Table 1). Scale bar, 10 μ m.

higher in thrombin-activated cells (lane 1) than in platelets bound to GST-rhodostomin (lane 3), given the relatively equal amount of FAK protein loaded in each lane (Fig. 6B).

Kinetic Events of Platelet Transformation

To compare the substrate effects of GST-rhodostomin and fibrinogen, we carefully examined the kinet-

TABLE 1

The Percentage of Full-Spreading Platelets on Different Concentrations GST-Rhodostomin-Coated Plates

| Concentration/ Exp | Experiment | | Average |
|------------------------|------------|---------|-----------|
| | 1 | 2 | |
| 1.6×10^{-9} M | 9/375 | 7/315 | 16/690 |
| | (2.40%) | (2.20%) | (2.31%) |
| 8×10^{-9} M | 105/456 | 57/399 | 162/855 |
| | (23.0%) | (14.3%) | (18.9%) |
| 4×10^{-8} M | 513/588 | 354/529 | 867/1117 |
| | (87.2%) | (66.9%) | (77.6%) |
| 2×10^{-7} M | 588/609 | 542/576 | 1130/1185 |
| | (93.6%) | (94.0%) | (95.4%) |

ics of cell transformation using time-lapse video microscopy. As shown in Fig. 7, most of the cells that adhered to the GST-rhodostomin substrate transformed into a pancake shape (Fig. 7A), while cells on the fibrinogen substrate were poorly attached and mostly round (Fig. 7E). Under a higher magnification, a freely moving cell was noted to become tightly adherent to the GST-rhodostomin-treated surface (Fig. 7B) and, within 5 min become fully spread (Fig. 7C). A few filopodia were noted to protrude during this period, together with the steady expansion of the peripheral lamella region (dashed box, Fig. 7C) at an average rate of $0.43 \mu\text{m}/\text{minute}$. (arrowheads, Fig. 7D). Note that after the cell had adopted a fully spread conformation,

very little dynamic activity of lamella was observed. In contrast, the cells interacting with fibrinogen surface remained loosely bound (Figs. 7F and 7G); neither outgrowth of filopodia nor significant advance of cell margin was observed (arrowheads, Fig. 7H). The cells on fibrinogen-coated substrates, however, could become fully spread by addition of 0.02 NIH unit/ml thrombin in the medium (Fig. 7I). Almost immediately after addition of the drug, the cells became adherent and then gradually flattened and spread (Figs. 7J and 7K). The processes of platelet spreading (Fig. 7L) were similar to those observed on GST-rhodostomin substrates; however, rates of filopodia outgrowth and lamella expansion were much slower. The average growth rate of lamella during the 420-s observation period was only $0.22 \mu\text{m}/\text{minute}$ (arrowheads, Fig. 7L), about half of the lamella expansion rate measured on GST-rhodostomin plates (Fig. 7D).

Active Calcium Oscillation during Platelet Transformation

Since calcium signaling has long been implicated in regulation of actin rearrangement and structural changes in the cell [44–46], we have carefully monitored changes in intracellular calcium concentration ($[\text{Ca}^{2+}]_i$) during platelet transformation. In our calcium imaging experiments, the nonratioed calcium indicator Calcium Green I was used to achieve the best temporal resolution at 30 frames/s. Cells loaded with calcium dye were typically plated on substrates and recorded

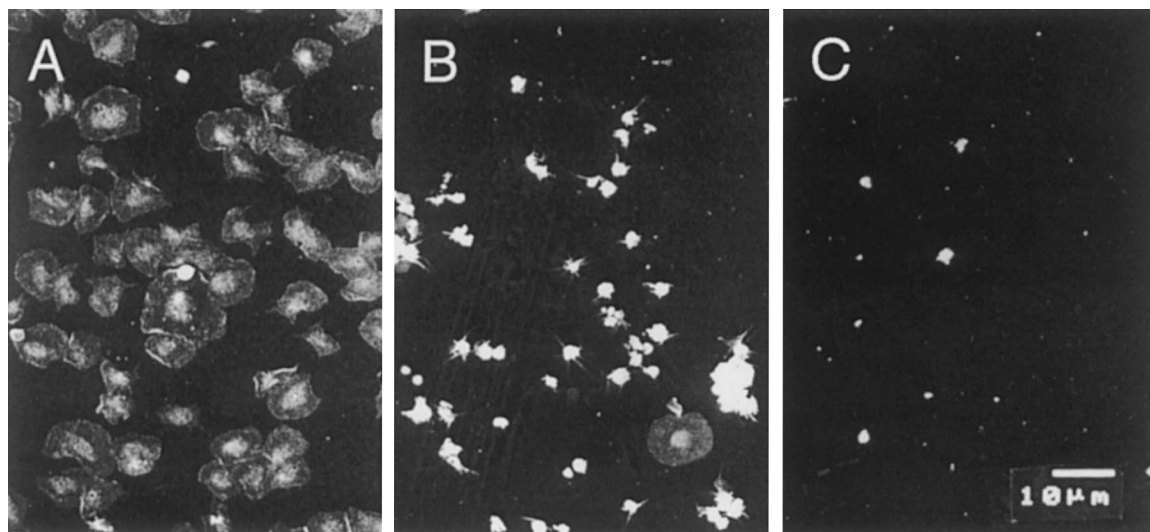


FIG. 4. SEM study of platelet transformation on different substrates. Freshly prepared human platelets were incubated with substrates coated with $20 \mu\text{g}/\text{ml}$ of GST-rhodostomin (A), fibrinogen (B), and bovine serum albumin (C) for 15 min before being processed for SEM examination. Although many flattened platelets were observed on the plate treated with rhodostomin, few, if any, spread cells were noted on the fibrinogen plates. No cell spreading was observed on the control substrate coated with BSA. Representative SEM fields from individual experimental conditions are shown. Scale bar, $10 \mu\text{m}$.

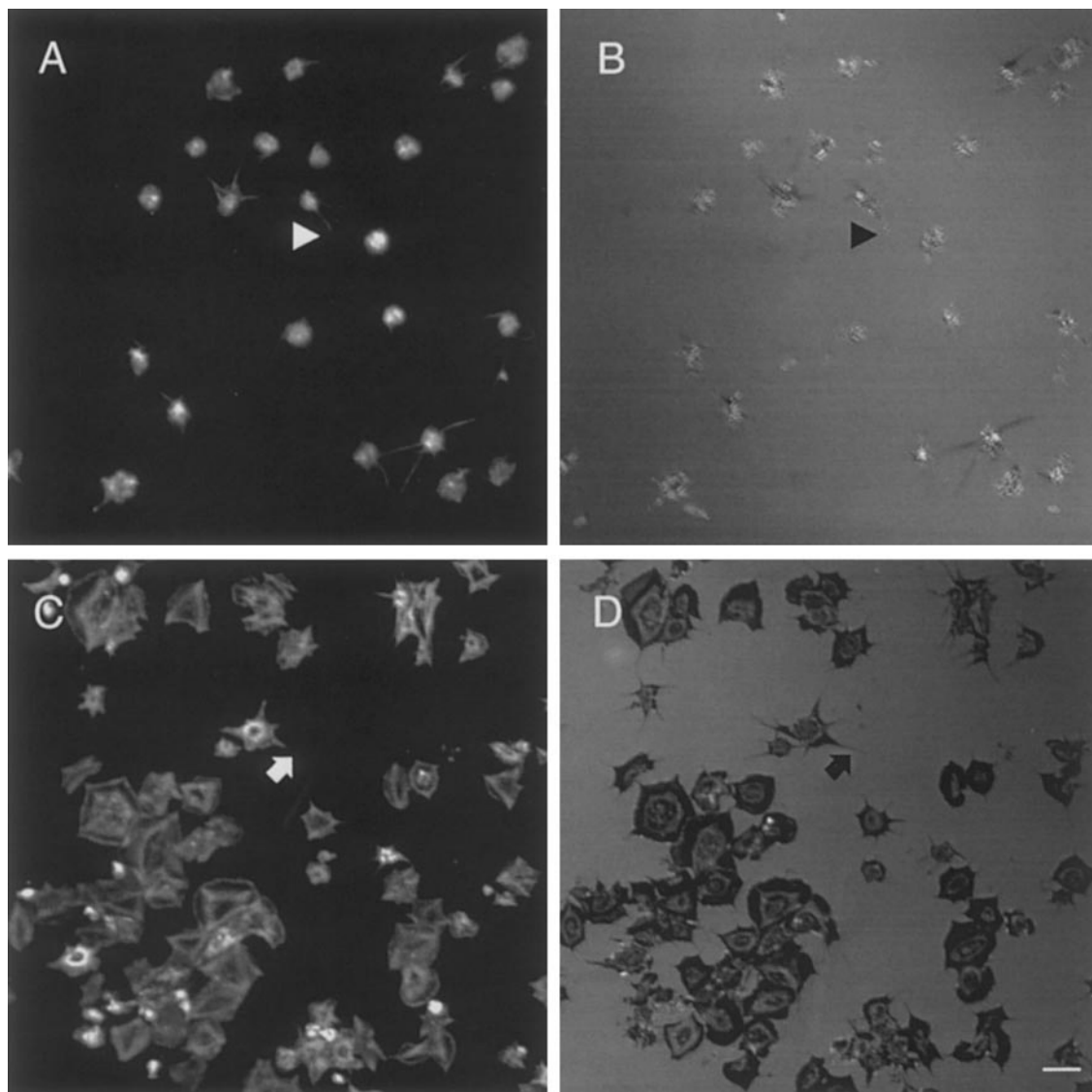


FIG. 5. Fully spread cells adhered more closely to the substrate. Platelets interacting with fibrinogen (A, B)- or GST-rhodostomin-coated substrates (C, D) were fixed and stained with rhodamine-phalloidin and then observed under fluorescence (A, C) and IRM (B, D) microscopy. Note that spread cells on the GST-rhodostomin plate appeared darker under IRM, indicating closer apposition between the cell and the underlying coverglass substrate (arrows). Cells plated on fibrinogen substrate, in contrast, exhibited bright patterns under IRM, suggesting that these cells were loosely bound (arrowheads). Scale bar, 10 μm .

under a fluorescence microscope that was optimized to reduce photobleaching. Figure 8A shows a typical field of flattened platelets on the GST-rhodostomin plates. Individual cells (Nos. 1–4, for examples) in this field exhibited differences of fluorescence intensity, indicating different states of calcium activity. The time sequences of calcium kinetics of cells 3 and 4 are shown in Fig. 8B. Note that a typical cycle of calcium oscillation was observed in cell 3, while $[\text{Ca}^{2+}]_i$ of cell 4 remained largely unchanged during the observation period.

Calcium oscillation activity varied among different

cells; some of them spiked as fast as 1 Hz, while others were inactive for a long period of time. As shown in Fig. 8C and Table 2, we have employed a new assay to calculate the frequency of calcium oscillation, where the slopes of fluorescence changes (indicative of calcium fluctuation) were plotted as a function of time (see Materials and Methods). In this analysis, we found that cell 1 exhibited two calcium spikes 1.7 s apart during the 2.5-s observation interval, whereas cell 2 showed only one spike; cell 3 had three and cell 4 possessed none. To calculate the average frequency of calcium oscillation in a cell

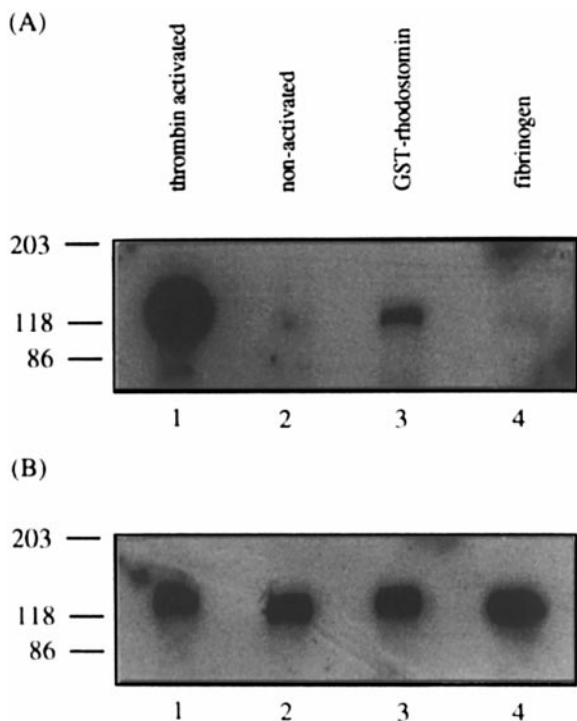


FIG. 6. FAK proteins were highly phosphorylated in platelets of rhodostomin plates. Total cell extracts from cells before (lane 2) and after (lane 1) 0.02 NIH unit/ml thrombin treatment or cells plated on GST-rhodostomin (lane 3) and fibrinogen (lane 4) substrates were subjected to immunoprecipitation using anti-FAK antibody. The precipitates were then separated by SDS-PAGE and blotted with anti-phosphotyrosine antibody (A). The same gel was also reprocessed to reveal FAK proteins using another anti-FAK antibody (B).

population, we sampled at least 120 cells, each observed for a 30-s period under each experimental condition (Table 2). The frequency of calcium oscillation was about 2.22 spike/cell/minute within platelets on BSA-coated plates and 2.76 spike/cell/minute on fibrinogen plates. On GST-rhodostomin substrates, the frequency of calcium oscillation increased to 4.77 spike/cell/minute, about 70% higher than the control rate on fibrinogen plates and more than two times higher than on BSA substrates. Since activated platelets could fully spread on fibrinogen substrates, we asked if these cells also had higher rates of calcium oscillation. In these experiments, we used ADP instead of thrombin to activate and induce platelet transformation because thrombin treatment was noted to raise intracellular calcium to a long-lasting plateau level that covered the oscillation activity (data not shown; see also [41]). We found that ADP-activated platelets on fibrinogen-coated substrates exhibited 9.09 spike/cell/minute calcium oscillation activity, about four times higher than the frequency of nonactivated platelets on fibrinogen plates.

DISCUSSION

In this study, we have established a novel approach to quantitating the rate of platelet spreading and the averaged frequency of calcium oscillation within platelets where the sample size is greater than 100 platelets (Figs. 7 and 8 and Table 2). The measured parameters are highly correlated with the state of platelet activities (Figs. 2–6). We propose that this approach should be used as a new indicator for future research in platelet activities. Additionally, this study has demonstrated that recombinant GST-rhodostomin is an ideal substrate for studying platelet adhesion.

Generally, native rhodostomin is a potent agent used to study anti-coagulation in solution [28, 29]; however, to our knowledge, it has never been used as a substrate for platelet adhesion. In solution, GST-rhodostomin has previously been demonstrated to inhibit ADP- and thrombin-induced platelet aggregation [30] and is unable to activate and transform platelets as shown in this study (Fig. 1). On a solid surface, immobilized GST-rhodostomin not only induces translocation of P-selectin from internal stores to the platelet surface (Fig. 2) but also induces sequential platelet spreading events (Fig. 7). These two different characteristics of GST-rhodostomin interacting with platelets merit an approach using the recombinant protein as a novel probe for platelet studies.

Using a combination of SEM, IRM, and high-resolution time-lapse video microscopy, this study has also provided a detailed description as well as dynamic measurements of the structural changes associated with platelet transformation (Figs. 3, 5, and 7). On GST-rhodostomin-coated plates, we found a steady and rapid outgrowth of filopodia and lamella, accompanied by close apposition between the cell and substrate. In contrast, the relatively quiescent cells on the fibrinogen plates displayed loose attachments to the substrates (Fig. 5). Compared with other cell outgrowth rates (ranging from 0.1 to 1.10 $\mu\text{m}/\text{minute}$; [47]), the lamellar advancing rate of platelets plated on GST-rhodostomin (0.43 $\mu\text{m}/\text{minute}$) is considered moderate. Note that this rate is almost twice as fast as that observed in thrombin-activated platelets on fibrinogen substrate (0.22 $\mu\text{m}/\text{minute}$). Without measuring the rate of platelet spreading, it would be impossible to discern two different platelet activities induced by GST-rhodostomin and thrombin. Generally speaking, the growth of cellular processes reflects the polymerization rate of intracellular actin, which is regulated by various signals and via various pathways [48, 49]. This observation indicates that although some effects of GST-rhodostomin substrate may be mimicked by the combination of thrombin/ADP activation and fibrino-

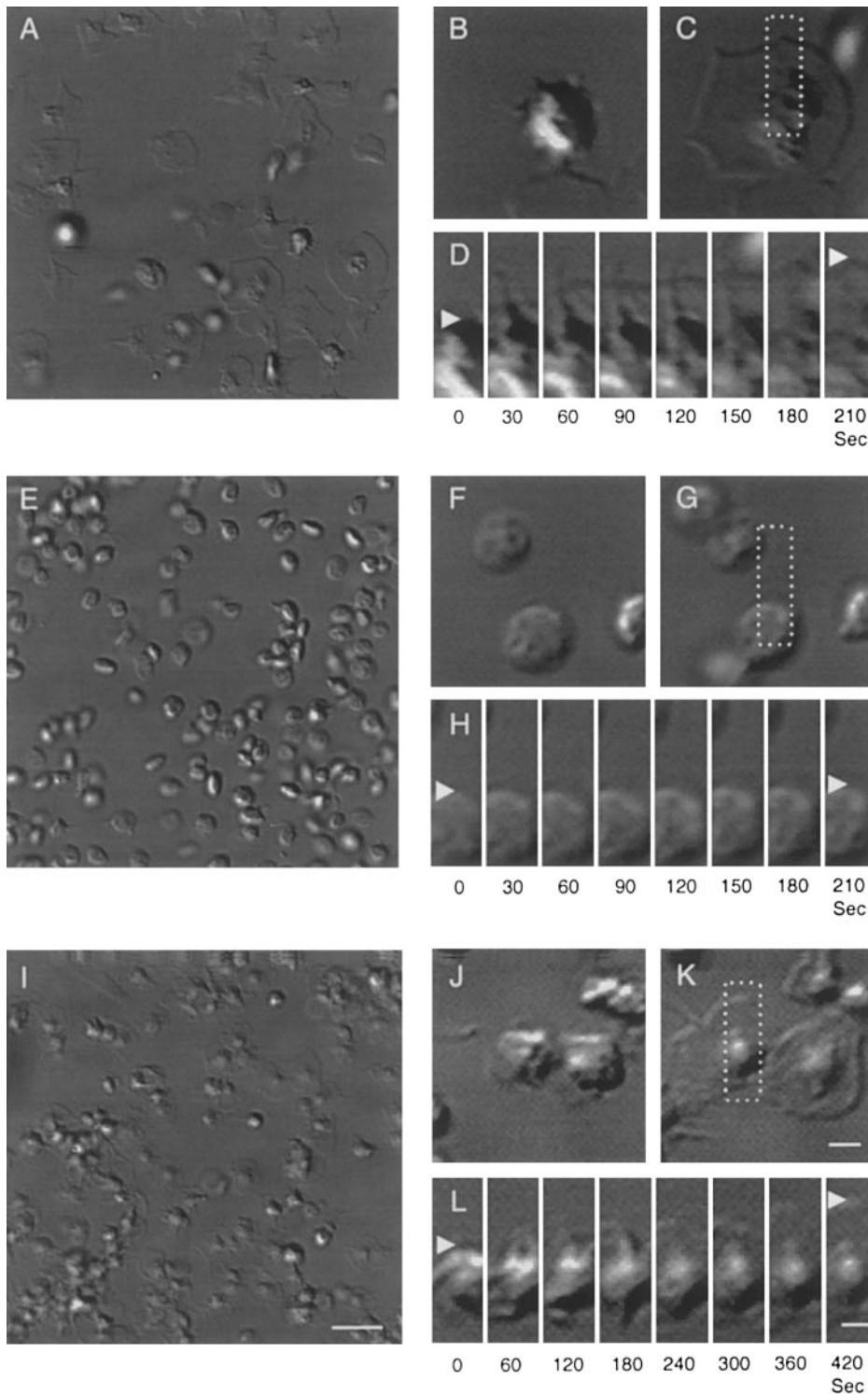


FIG. 7. DIC sequence of platelet transformation on various substrates. (A–D) Cells adhering to GST–rhodostomin substrates typically exhibited fully spread conformation after 15 min of incubation (A). On this plate, a cell (arrowheads) was noted to contact the substrate (B) and then became fully spread within 3.5 min (C). Time-lapse recording of the peripheral lamella (dashed box) revealed a steady extension at an average rate of $0.43 \mu\text{m}/\text{minute}$ (D). (E–H) Platelets plated on the fibrinogen-coated substrate, in contrast, did not exhibit significant cell flattening (E). They contacted the substrate (F) but remained loosely bound for the subsequent 3.5 min (G). No significant outgrowth of filopodia or lamellipodium was noted (H). (I–K) The loosely attached platelets on fibrinogen substrates became adherent and fully spread after addition of 0.02 NIH unit/ml thrombin (I). The morphological transformation (J–K) was similar to that observed on the GST–rhodostomin plate, although lamella expansion (L) was much slower (average $0.22 \mu\text{m}/\text{minute}$). The scale bar is equal to $10 \mu\text{m}$ in A, E, and I and $2 \mu\text{m}$ in other panels. Time intervals for the sequences are shown.

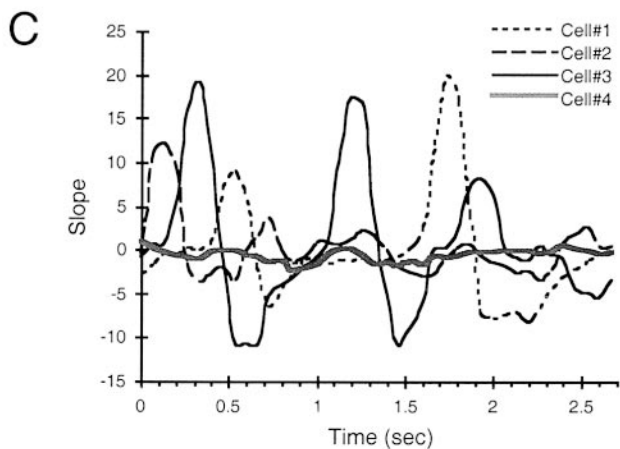
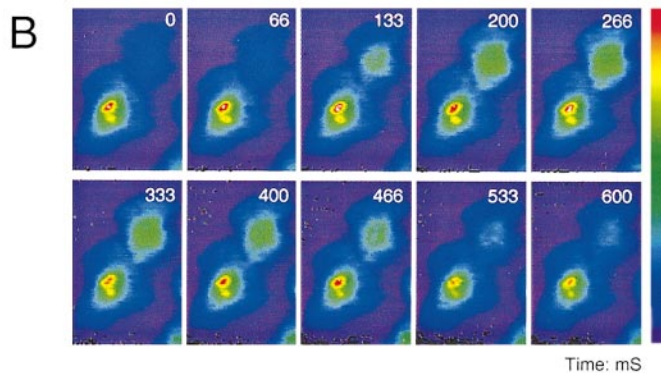
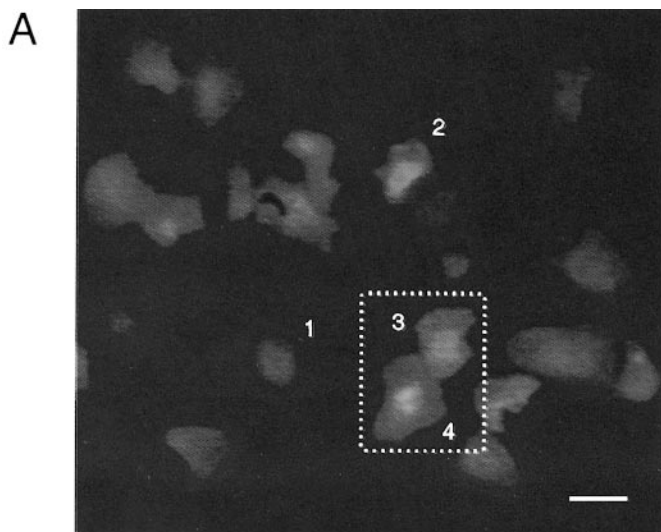


FIG. 8. Calcium oscillations within platelets on the GST-rhodostomin-coated substrate. (A) Platelets loaded with Calcium Green I were incubated on GST-rhodostomin substrates for 30 min and observed under a fluorescence microscope. Note that most cells had already adopted fully spread conformations. (B) The changes in intracellular calcium concentration in cells 3 and 4 (dashed box) were further analyzed at a temporal resolution of 15 frames/s. Note that cell 3 exhibited a typical cycle of calcium spike, while cell 4 remained largely unchanged. The time sequence is indicated in millisecond

TABLE 2

The Calcium Oscillation Frequency of Platelet Adhesion on Different Protein-Coated Plates (Spike/Cell/Min)

| Condition/Exp | Experiment | | Average |
|---------------|------------|------|---------|
| | 1 | 2 | |
| BSA | 2.70 | 1.74 | 2.22 |
| FB | 3.54 | 1.98 | 2.76 |
| FB + ADP | 10.86 | 7.32 | 9.09 |
| Rhodostomin | 5.64 | 3.90 | 4.77 |

gen surfaces, their underlying mechanisms and signaling pathways are probably not identical.

With regard to the investigation of calcium signaling during platelet transformation, we present a novel approach to quantitating oscillations within a single as well as within a population of platelets (Fig. 8 and Table 2; cf. [50, 51]). Previously, the change in calcium ion concentration ($[Ca^{2+}]_i$) in activated platelets was measured by either a population of cells or an individual cell [52, 53]. Our current results are consistent with the previous finding that the $[Ca^{2+}]_i$ response to stimulation greatly differed among individual cells [53]; i.e., some are inert and some are highly fluctuated (Fig. 8). Although the reason for various $[Ca^{2+}]_i$ changes in a population of cells under the same condition is unknown, we proposed that the unit of spike/cell/minute formulated in this study reflects more accurate calcium oscillations in a population of cells. Using this new formulation, we found very active calcium oscillation activity that fluctuated as fast as 1 Hz during platelet transformation on a GST-rhodostomin substrate or on fibrinogen plates after ADP treatment. Without using this new method for measuring calcium oscillations, it would be impossible to distinguish the level of platelet activity when platelets adhere on fibrinogen-coated plates in the presence or the absence of ADP (9.09 spike/cell/minute vs 2.76 spike/cell/minute) (Table 2). The molecular mechanisms of this calcium activity remain largely unknown; however, our preliminary results suggested the involvement of ER and other internal calcium stores since thapsigargin treatment effectively inhibited calcium oscillations.

Platelet activation can occur via stimulation of various agonists, such as thrombin and ADP. Extracellu-

(mS). (C) The degree of fluorescence fluctuation (see Materials and Methods) was plotted as a function of time. Note that individual cells (numbered from panel A) possessed different rates of calcium oscillation during the 2.75-s observation period. Scale bar, 5 μ m.

lar matrices with an RGD-containing motif, such as fibronectin, vitronectin, and osteopontin, induce platelet adhesion and spreading via binding to the integrin $\alpha_{\text{IIb}}\beta_3$ receptor [2, 18]. All stimuli finally target the phosphorylation of FAK and the reorganization of actin, to result in platelet transformation [54, 55]. The results in Fig. 6 show that the degree of FAK phosphorylation within platelets activated by GST-rhodostomin was only about one third the level after thrombin activation, suggesting again that the signal transduction pathways for GST-rhodostomin and thrombin may not be totally identical and other associated molecules may be involved. Various rates of lamellar advancing and degrees of platelet transformation observed on different substrates mirror the polymerization of intracellular actin which could be mediated by different small G-proteins, such as Cdc42, Rac, and Rho, as reported in fibroblast cells [49, 56].

In some aspects, the substrate effects of GST-rhodostomin were more like those of fibronectin than fibrinogen. Platelets could bind to either fibronectin- or fibrinogen-coated surfaces and resulted in formation of specific structures at cell attachment sites called protected zones of adhesion (PZA), which are capable of excluding plasma proteins [57, 58]. The fibronectin substrate alone could cause over 70% of the cells to form PZA, whereas only 26% of cells formed PZA on the fibrinogen plates. Similar to our finding, addition of thrombin/ADP to fibrinogen plates enhanced the extent of PZA formation to over 80% [57]. Although both GST-rhodostomin and fibronectin can bind to integrin $\alpha_{\text{IIb}}\beta_3$, fibronectin is much larger than rhodostomin and has functional motifs other than RGD for binding to other species of integrins, i.e., $\alpha_5\beta_1$ [19]. It is possible that the structure surrounding the RGD binding motif are also important in modulating the functions of rhodostomin. To address this question, an obvious approach is to employ site-directed mutagenesis techniques to dissect the rhodostomin molecule [59–61]. The structural biology information will be meaningful only when integrated with the functions of the molecule. The current research has provided important functional assays to actively access platelet activation and transformation events. It is hoped that by using recombinant rhodostomin as a probe, we can learn additional molecular details about human platelet activities that are central to the functions of hemostasis and thrombosis.

We gratefully acknowledge inspiration and valuable comments from Drs. M. T. Hsu and T. Y. Chen of NYMU. We are grateful to Dr. J. D. Taylor of WSU for his valuable comments on revising the manuscript. Special thanks also to the EM and confocal microscopy facility of NYMU and to Weber Chen for the wonderful technical help. This work was supported by grants from the National Science Council (NSC87-2314-B-010-128) and the National Health Research

Institute (DOH87-HR-733) to C.H.L. and by NSC85-2331-B-010-002 and NSC86-2314-B-010-026 awarded to S.J.L.

REFERENCES

- Kroll, M. H., and Schafer, A. I. (1989). Biochemical mechanisms of platelet activation. *Blood* **74**, 1181–1195.
- Shattil, S. J., Ginsberg, M. H., and Brugge, J. S. (1994). Adhesive signaling in platelets. *Curr. Opin. Cell Biol.* **6**, 695–704.
- Leung, L. L. K., and Nachman, R. L. (1986). Molecular mechanisms of platelet aggregation. *Annu. Rev. Med.* **37**, 179–186.
- Alexandrova, A. Y., and Vasiliev, J. M. (1984). Focal contacts of spreading platelets with the substratum. *Exp. Cell Res.* **153**, 254–258.
- Fox, J. E. B. (1986). The platelet cytoskeleton. In "Thrombosis and Haemostasis" (M. Verstraete, J. Vermeylen, R. Lijnen, and J. Arnout, Eds.), Leuven Univ. Press, Leuven, Belgium.
- Haimovich, B., Lipfert, L., Brugge, J. S., and Shattil, S. J. (1993). Tyrosine phosphorylation and cytoskeletal reorganization in platelets are triggered by interaction of integrin receptors with their immobilized ligands. *J. Biol. Chem.* **268**, 15868–15877.
- Winokur, R., and Hartwig, J. H. (1995). Mechanism of shape change in chilled human platelets. *Blood* **85**, 1796–1804.
- Savage, B., Saldivar, E., and Ruggeri, Z. M. (1996). Initiation of platelet adhesion by arrest onto fibrinogen or translocation on von Willebrand factor. *Cell* **84**, 289–297.
- Schwartz, M. A., Schaller, M. D., and Ginsberg, M. H. (1995). Integrins: Emerging paradigm of signal transduction. *Annu. Rev. Cell Biol. Dev. Biol.* **11**, 549–600.
- Shattil, S. J., Kashiwagi, H., and Pampori, N. (1998). Integrin signaling: The platelet paradigm. *Blood* **91**, 2645–2657.
- Haimovich, B., Kaneshiki, N., and Ji, P. (1996). Protein kinase C regulates tyrosine phosphorylation of pp125 FAK in platelets adherent to fibrinogen. *Blood* **87**, 152–161.
- Rink, T. J., and Sage, S. O. (1990). Calcium signalling in human platelets. *Annu. Rev. Physiol.* **52**, 431–449.
- Hartwig, J. H., and DeSisto, M. (1991). The cytoskeleton of the resting human blood platelet: Structure of the membrane skeleton and its attachment to actin filaments. *J. Cell Biol.* **112**, 407–425.
- Weisel, J. W., Nagaswami, C., Vilaire, G., and Bennett, J. S. (1992). Examination of the platelet membrane glycoprotein IIb-IIIa complex and its interaction with fibrinogen and other ligands by electron microscopy. *J. Biol. Chem.* **267**, 16637–16643.
- Savage, B., Shattil, S. J., and Ruggeri, Z. M. (1992). Modulation of platelet function through adhesion receptors. A dual role for glycoprotein IIb-IIIa (integrin $\alpha_{\text{IIb}}\beta_3$) mediated by fibrinogen and glycoprotein Ib-von Willebrand factor. *J. Biol. Chem.* **267**, 11300–11306.
- Hung, D. T., Vu, T.-K. H., Wheaton, V. I., Ishii, K., and Coughlin, S. R. (1992). Cloned platelet thrombin receptor is necessary for thrombin-induced platelet activation. *J. Clin. Invest.* **89**, 1350–1353.
- Gachet, C., Hechler, B., Leon, C., Vial, C., Leray, C., Ohlmann, P., and Cazenave, J. P. (1997). Activation of ADP receptors and platelet function. *Thromb. Haemostasis* **78**, 271–275.
- Hynes, R. O. (1992). Integrins: versatility, modulation, and signalling in cell adhesion. *Cell* **69**, 11–25.
- Ginsberg, M. H., Du, X., and Plow, E. F. (1992). Inside-out integrin signaling. *Curr. Opin. Cell Biol.* **4**, 766–771.

20. Ugrova, T. P., Budzynski, A. Z., Shattil, S. J., Ruggeri, Z. M., Ginsberg, M. H., and Plow, E. F. (1993). Conformational changes in fibrinogen elicited by its interaction with platelet membrane glycoprotein GPIIb-IIIa. *J. Biol. Chem.* **268**, 21080–21087.
21. Bazzoni, G., and Hemler, M. E. (1998). Are changes in integrin affinity and conformation overemphasized? *Trends Biochem. Sci.* **23**, 30–34.
22. Savage, B., Bottini, E., and Ruggeri, Z. M. (1995). Interaction of integrin $\alpha_{Ib}\beta_3$ with multiple fibrinogen domains during platelet adhesion. *J. Biol. Chem.* **270**, 28812–28817.
23. Smith, J. W., Piotrowicz, R. S., and Mathis, D. (1994). A mechanism for divalent cation regulation of β_3 -integrins. *J. Biol. Chem.* **269**, 960–967.
24. Gould, R. J., Polokoff, M. A., Friedman, P. A., Huang, T. F., Holt, J. C., Cook, J. J., and Niewiarowski, S. (1990). Disintegrins: a family of integrin inhibitory proteins from viper venoms. *Proc. Soc. Exp. Biol. Med.* **195**, 168–171.
25. Huang, T.-F., and Niewiarowski, S. (1994). Disintegrins: The naturally-occurring antagonists of platelet fibrinogen receptor. *J. Toxicol. Toxin Rev.* **13**, 253–273.
26. Adler, M., Lazarus, R. A., Dennis, M. S., and Wagner, G. (1991). Solution structure of kistrin, a potent platelet aggregation inhibitor and GP IIB-IIIa antagonist. *Science* **253**, 445–448.
27. Huang, T.-F., Wu, Y. J., and Ouyang, C. (1987). Action mechanism of the platelet aggregation inhibitor from *Agkistrodon rhodostoma* snake venom. *Biochim. Biophys. Acta* **925**, 248–257.
28. Teng, C.-M., and Huang, T.-F. (1991). Inventory of exogenous inhibitors of platelet aggregation. *Throm. Haemostasis* **65**, 624–626.
29. Teng, C.-M., and Huang, T.-F. (1991). Snake venom constituents that affect platelet function. *Platelets* **2**, 77–87.
30. Chang, H.-H., Tsai, W. J., and Lo, S. J. (1997). Glutathione S-transferase-rhodostomin fusion protein inhibits platelet aggregation and induces platelet shape change. *Toxicol* **35**, 195–204.
31. Chang, H.-H., and Lo, S. J. (1998). Full-spreading platelets induced by the recombinant rhodostomin are via binding to integrins and correlated with FAK phosphorylation. *Toxicol* **36**, 1087–1099.
32. Smith, D. B., and Johnson, K. S. (1988). Single-step purification of polypeptides expressed in *Escherichia coli* as fusion with glutathione S-transferase. *Gene* **67**, 31–38.
33. Laemmli, U. K. (1970). Cleavage of structural proteins during the assembly of the head of bacteriophage T4. *Nature* **227**, 680–685.
34. Lo, S. J., Taylor, J. D., and Tchen, T. T. (1979). ACTH-induced internalization of plasma membrane in xanthophores of the goldfish, *Carassius auratus* L. *Biochem. Biophys. Res. Commun.* **86**, 748–754.
35. Curtis, A. S. G. (1964). The mechanism of adhesion of cells to glass. *J. Cell Biol.* **20**, 199–215.
36. Letourneau, P. C. (1981). Immunocytochemical evidence for colocalization in neurite growth cones of actin and myosin and their relationship to cell-substratum adhesions. *Dev. Biol.* **85**, 113–122.
37. Towbin, H., Staehelin, T., and Gordon, J. (1979). Electrophoretic transfer of proteins from polyacrylamide gels to nitrocellulose sheets: procedure and some applications. *Proc. Natl. Acad. Sci. USA* **76**, 4350–4354.
38. Lipfert, L., Haimovich, B., Schaller, M. D., Cobb, B. S., Parsons, J. T., and Brugge, J. S. (1992). Integrin-dependent phosphorylation and activation of the protein tyrosine kinase pp125^{FAK} in platelets. *J. Cell Biol.* **119**, 905–912.
39. Shattil, S. J., Haimovich, B., Cunningham, M., Lipfert, L., Parsons, J. T., Ginsberg, M. H., and Brugge, J. S. (1994). Tyrosine phosphorylation of pp125^{FAK} in platelets requires coordinated signaling through integrin and agonist receptor. *J. Biol. Chem.* **269**, 14738–14745.
40. Lin, C.-H., Espreafico, E. M., Mooseker, M. S., and Forscher, P. (1996). Myosin drives retrograde F-actin flow in neuronal growth cones. *Neuron* **16**, 769–782.
41. Markram, H., and Sakmann, B. (1994). Calcium transients in dendrites of neocortical neurons evoked by single threshold excitatory postsynaptic potentials via low-voltage-active calcium channels. *Proc. Natl. Acad. Sci. USA* **91**, 5207–5211.
42. Michelson, A. D., and Shattil, S. J. (1996). The use of flow cytometry to study platelet activation. In "Platelets: A Practical Approach" (S. P. Watson and K. S. Authi, Eds.), IRL Press, Oxford.
43. Burridge, K., Turner, C. E., and Romer, L. H. (1992). Tyrosine phosphorylation of paxillin and pp125^{FAK} accompanies cell adhesion to extracellular matrix: A role in cytoskeletal assembly. *J. Cell Biol.* **119**, 893–903.
44. Zobel, C. R., and Woods, A. (1983). Effect on calcium on the morphology of human platelets spread on glass substrates. *Eur. J. Cell Biol.* **30**, 83–92.
45. Stossel, T. P. (1993). On the crawling of animal cells. *Science* **260**, 1086–1094.
46. Jen, C. J., Chen, H.-I., Lai, K.-C., and Usami, S. (1996). Changes in cytosolic calcium concentrations and cell morphology in single platelets adhered to fibrinogen-coated surface under flow. *Blood* **87**, 3775–3782.
47. Lin, C.-H., and Forscher, P. (1993). Cytoskeletal remodeling during growth cone-target interactions. *J. Cell Biol.* **121**, 1369–1383.
48. Clark, E. A., and Brugge, J. S. (1995). Integrins and signal transduction pathways: the road taken. *Science* **268**, 233–239.
49. Schoenwaelder, S. M., and Burridge, K. (1999). Bidirectional signaling between the cytoskeleton and integrins. *Curr. Opin. Cell Biol.* **11**, 274–286.
50. Heemskerk, J. W., Hoyland, J., Mason, W. T., and Sage, S. O. (1992). Spiking in cytosolic calcium concentration in single fibrinogen-bound fura-2-loaded human platelets. *Biochem. J.* **283**, 379–383.
51. Heemskerk, J. W., Vis, P., Feijge, M. A., Hoyland, J., Mason, W. T., and Sage, S. O. (1993). Roles of phospholipase C and Ca²⁺-ATPase in calcium responses of single, fibrinogen-bound platelets. *J. Biol. Chem.* **268**, 356–363.
52. Nishio, H., Ikegami, Y., and Segawa, T. (1991). Fluorescence digital image analysis of serotonin-induced calcium oscillations in single blood platelets. *Cell Calcium* **12**, 177–184.
53. Ozake, Y., Yatomi, Y., Wakasugi, S., Shirasawa, Y., Satio, H., and Kume, S. (1992). Thrombin-induced calcium oscillation in human platelets and MEG-01, a megakaryoblastic leukemia cell line. *Biochem. Biophys. Res. Commun.* **183**, 864–871.
54. Fox, J. E., Lipfert, L., Clark, E. A., Reynolds, C. C., Austin, C. D., and Brugge, J. S. (1993). On the role of the platelet membrane skeleton in mediating signal transduction: Association of GP IIB-IIIa, pp60c-src, pp62c-yes, and the p21ras GTPase-activating protein with the membrane skeleton. *J. Biol. Chem.* **268**, 25973–25984.

55. Pelletier, A. J., Kunicki, T., Ruggeri, Z. M., and Quaranta, V. (1995). The activation state of the integrin alpha IIB beta 3 affects outside-in signals leading to cell spreading and focal adhesion kinase phosphorylation. *J. Biol. Chem.* **270**, 18133–18140.
56. Nobles, C. D., and Hall, A. (1995). Rho, Rac, and Cdc42 GTPases regulate the assembly of multimolecular focal complexes associated with actin stress fiber, lamellipodia, and filopodia. *Cell* **81**, 53–62.
57. Loike, J. D., Silverstein, R., Cao, L., Solomon, L., Weitz, J., Haber, E., Matsueda, G. R., Bernatowicz, M. S., and Silverstein, S. C. (1993). Activated platelets form protected zones of adhesion on fibrinogen and fibronectin-coated surfaces. *J. Cell Biol.* **121**, 945–955.
58. Tourkin, A., Bonner, M., Mantrova, E., LeRoy, E. C., and Hoffman, S. (1996). Dot-like focal contacts in adherent eosinophils, their redistribution into peripheral belts, and correlated effects on cell migration and protected zone formation. *J. Cell Sci.* **109**, 2169–2177.
59. Dennis, M. S., Carter, P., and Lazarus, R. A. (1993). Binding interactions of kistrin with platelet glycoprotein IIB-IIIa: analysis by site-directed mutagenesis. *Proteins: Struct. Funct. Genet.* **15**, 312–321.
60. Lu, X., Rahman, S., Kakkar, V. V., and Authi, K. S. (1996). Substitutions of prolines 42 to alanine and methionine 46 to asparagine around the RGD domain of the neurotoxin dendroaspil alter its preferential antagonism to that resembling the disintegrin elegantin. *J. Biol. Chem.* **271**, 289–294.
61. Zhang, X.-P., Kamata, T., Yokoyama, K., Puzon-McLaughlin, W., and Takada, Y. (1998). Specific interaction of the recombinant disintegrin-like domain of MDC-15 (metargidin, ADAM-15) with integrin $\alpha_v\beta_3$. *J. Biol. Chem.* **273**, 7345–7350.

Received September 29, 1998

Revised version received April 22, 1999